ChemBioChem

Research Article
doi.org/10.1002/cbic.202200069

Chemistry Europe
European Chemical Societies Publishing

www.chembiochem.org

Carbonate-Based Fluorescent Chemical Tool for Uncovering Carboxylesterase 1 (CES1) Activity Variations in Live Cells

Anchal Singh,[a] Mingze Gao,[b] Carolyn J. Karns,[b] Taylor P. Spidle,[b] and Michael W. Beck*[a]

Carboxylesterase 1 (CES1) plays a key role in the metabolism of endogenous biomolecules and xenobiotics including a variety of pharmaceuticals. Despite the established importance of CES1 in drug metabolism, methods to study factors that can vary CES1 activity are limited with only a few suitable for use in live cells. Herein, we report the development of FCP1, a new CES1 specific fluorescent probe with a unique carbonate substrate constructed from commercially available reagents. We show that FCP-1 can specifically report on endogenous CES1 activity with a robust fluorescence response in live HepG2 cells through studies with inhibitors and genetic knockdowns. Subsequently, we deployed FCP-1 to develop a live cell fluorescence microscopy-based approach to identify activity differences between CES1 isoforms. To the best of our knowledge, this is the first application of a fluorescent probe to measure the activity of CES1 sequence variants in live cells.

Introduction

Carboxylesterases (CESs) are members of the α/β-hydrolase superfamily.[1,2] The two main human CESs, carboxylesterase 1 (CES1) and carboxylesterase 2 (CES2), play a key role in the metabolism of many ester containing pharmaceuticals across different drug types including the first FDA approved antiviral treatment for COVID-19, remdesivir.[1–5] Carboxylesterase activity is known to vary between individuals due to a variety of genetic and environmental factors.[1,5,6] This is particularly true for CES1 where different clinical outcomes have been reported upon treatment with substrate drugs due to interindividual variability of CES1 activity caused by amino acid sequence differences.[1,5,6] Despite the importance of CES1 in drug metabolism, the factors that influence the activity of CES1 remain understudied compared to other enzymes involved in drug metabolism.[1,5,7]

To address this issue, a few fluorescent chemical tools capable of reporting on CES1 activity in live cells using fluorescence microscopy have been developed.[1,8–10] To date, these tools have been limited in use to study the factors that influence CES1 activity in live cells and the best characterized chemical tools, which have the highest potential utility, have been confined to the BODIPY framework due to their mechanism of reporting on CES1 activity.[1,8–12] Additionally, these probes require multiple synthetic steps to obtain. We sought to create a design approach that could be applied to a wider range of fluorophores, including those that are commercially available, to generate new fluorescent chemical tools to study CES1. Furthermore, we desired to use these tools to develop methods to explore the factors that influence CES1 activity in live cells. We believe expanding the availability and accessibility of chemical tools and methods to study CES1 will result in a better understanding of interindividual variations in CES1 activity.

Results and Discussion

CES1 and CES2 are known to have different substrate preferences primarily based on the observed metabolism of various pharmaceuticals.[1,6,13] CES1 generally prefers to hydrolyze esters consisting of a large carboxylic acid and a small alcohol similar to oseltamivir, a known CES1 substrate (Figure 1, left).[1,6,13] Conversely, CES2 generally prefers to hydrolyze esters consisting of a small carboxylic acid and a large alcohol such as the acetyl ester of aspirin (Figure 1, right).[1,6,13]

To generate new chemical tools that can monitor CES1 activity in live cells, we exploited the known self-immolative properties of carbonate groups to detect CES1 activity.[14] To enhance specificity for CES1 over CES2, we developed a carbonate substrate that we coin as a CES Janus substrate (Figure 1). This CES Janus substrate, named after the two-faced Roman god Janus, is rationally designed to impart preference for hydrolysis by CES1 over CES2 through presenting different substrate "faces" to CES1 and CES2. When our Janus substrate interacts with CES1, the substrate is designed to appear like the preferred ester with a large carboxylic acid and a small alcohol. Interaction with CES2, however, will appear to be an ester consisting of a large alcohol and an intermediate-sized carboxylic acid. This should reduce CES2's preference for our Janus substrate. Therefore, by presenting different "faces" to CES1 and CES2 this substrate is designed to enhance hydrolysis by CES1 while reducing hydrolysis by CES2.

To develop a fluorescent chemical tool, we decided to incorporate our CES Janus substrate into a xanthene fluorophore framework. This framework was chosen because it is

[a] A. Singh, Prof. Dr. M. W. Beck
Department of Chemistry and Biochemistry
Eastern Illinois University
Charleston, IL 61920 (USA)
E-mail: mbeck2@eiu.edu
[b] M. Gao, C. J. Karns, T. P. Spidle
Department of Biological Sciences
Eastern Illinois University
Charleston, IL 61920 (USA)

Supporting information for this article is available on the WWW under https://doi.org/10.1002/cbic.202200069

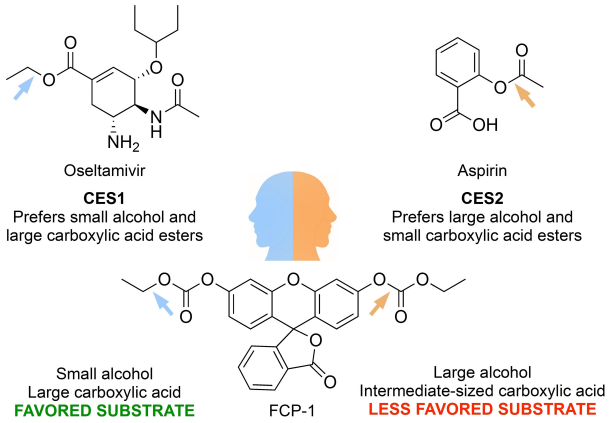

Figure 1. Substrate specificity of CESs and diagram of design strategy for carbonate based CES1 substrate. CES1 prefers esters consisting of a small alcohol and large carboxylic acid like known substrate oseltamivir. CES2 prefers esters consisting of a large alcohol and a small carboxylic acid like known substrate aspirin. Our CES1 Janus substrate can present different "faces" to CES1 and CES2. To CES1, the Janus substrate appears to have a small alcohol and large carboxylic acid, the preferred properties of a substrate for CES1. In contrast, this Janus substrate can appear to have a large alcohol and an intermediate-sized carboxylic acid to CES2 which should reduce CES2's hydrolysis of the substrate. Arrows indicate the preferred bond cleaved upon hydrolysis by CES1 or CES2.

well-established that the fluorescence properties of many xanthene fluorophores are sensitive to substitutions on the phenolic oxygen.[15–20] Fluorescein is a commercially available xanthene dye and has favorable fluorescent properties for live cell fluorescence microscopy. At physiological pH, it is highly fluorescent ($\Phi = 0.92$; $\varepsilon = 9.3 \times 10^4\ M^{-1}\,cm^{-1}$) with excitation and emission wavelengths in range of commonly available fluorescence filter sets.[19,21] Furthermore, fluorescein is water soluble and non-toxic having been used clinically in a variety of diagnostic applications since 1931.[22] Thus, we appended our CES Janus substrate to the 3′ and 6′ oxygens of fluorescein to create FCP-1 (Scheme 1). When the substrate is intact before cleavage, it holds FCP-1 in the nonfluorescent lactone form. CES1 hydrolysis demasks the carbonate initiating the self-immolation process to release fluorescein which allows the lactone to open into the highly fluorescent carboxylate form

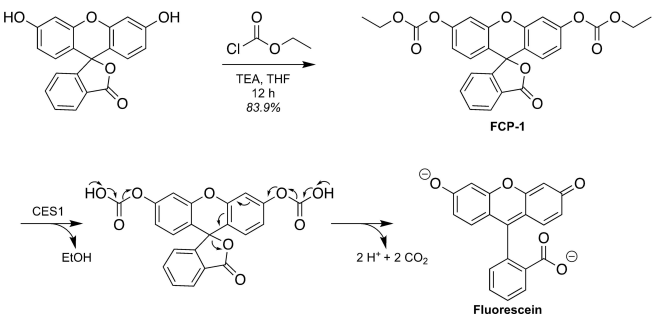

Scheme 1. Synthesis and CES1-mediated hydrolysis of FCP-1. FCP-1 was synthesized from fluorescein in one step. Hydrolysis of FCP-1 produces a short-lived intermediate which spontaneously rearranges to release carbon dioxide and fluorescein.

(Scheme 1). FCP-1 was synthesized from commercially available fluorescein and ethyl chloroformate in one step with high yield.

As designed, FCP-1 has limited absorbance and fluorescence properties (Figure S1). When the carbonate is removed, fluorescein is released producing a broad absorption with a maxima of 488 nm and excitation at this wavelength results in an emission with a maximum wavelength of 512 nm. We then determined the solution stability of FCP-1 in comparison to known *in vitro* CES2 substrate fluorescein diacetate (FDA).[23] No fluorescence from FCP-1 was observed during the first hour of incubation with less than 1% hydrolyzing into a fluorescent form after three hours of incubation at pH 7.4 (Figure 2A). The carbonate groups of FCP-1 were also determined to be more stable than the acetate groups of FDA at pH 7.4 with more than 4% hydrolyzing into a fluorescent form after three hours (Figure 2A). Additionally, both FCP-1 and FDA were stable in solution from pH 2.0 to 8.0 (Figure 2B). These results demonstrate that FCP-1 does not produce fluorescence signal in the absence of CESs under physiological conditions.

We next evaluated if our design strategy resulted in greater hydrolysis of FCP-1 by CES1. Studying this *in vitro* can be difficult as recombinant CES1 activity is known to vary depending on the method of purification.[24,25] Thus, purified CES1 may not accurately reflect actual CES1 activity in live systems potentially due to a variety of factors that could modulate CES1 activity including missing key post-translational modifications and interactions with other biomolecules.[1,24,25] To aid reproducibility and allow for comparison, we utilized commercially available preparations of CES1 and CES2 as well as normalized the activity of these enzymes by using the same units of activity instead of total protein. Additionally, we compared the hydrolysis of FCP-1 to FDA.[23] FDA has the same fluorophore

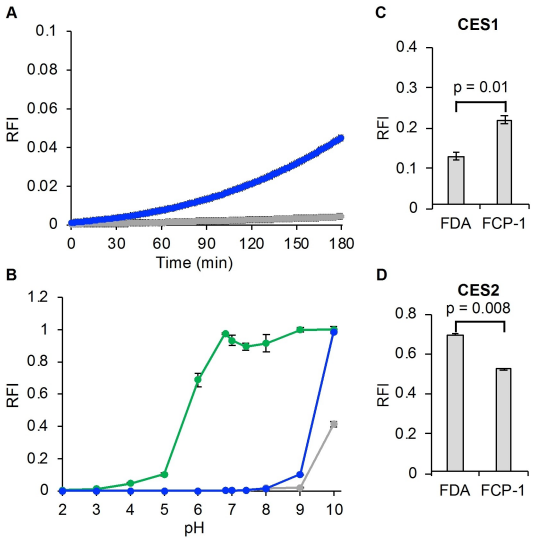

Figure 2. A. Stability of FCP-1 (gray) and FDA (blue) at pH 7.4 in 20 mM PBS. B. Stability of FCP-1 (gray) and FDA (blue) compared to the fluorescence of fluorescein (green) in various pH solutions. Relative fluorescence intensity after 15 minutes treatment of 1 μM FCP-1 or FDA with 1.7 units of C. CES1 or D. CES2 in PBS at pH 7.4. Error bars are ± std. dev. (n = 3). RFI = Relative Fluorescence Intensity to fluorescein. Error bars are ± std. dev. (n = 3).

core as FCP-1, but instead of the carbonate groups, FDA has two acetyl esters which are preferentially cleaved by CES2 *in vitro*.[23] This allowed us to understand the hydrolysis of FCP-1 in context of the hydrolysis of a structurally similar, but CES2-specific probe. Incubating FCP-1 with both CES1 and CES2 resulted in fluorescence indicating that both enzymes can hydrolyze FCP-1 (Figure 2C,D, S2, and S3). Comparison of the hydrolysis of FCP-1 to FDA revealed the use of the ethyl carbonate group in FCP-1 increases hydrolysis by CES1 while also decreasing hydrolysis by CES2 in comparison to the CES2-substrate acetate group of FDA with the ratio of hydrolysis by CES1:CES2 of FCP-1 being approximately double (0.41 +/− 0.02) of FDA (0.21 +/− 0.01) after 15 minutes. This indicates that our design strategy using an ethyl carbonate substrate was successful in increasing hydrolysis towards CES1 while decreasing hydrolysis by CES2.

To evaluate specificity for CES1 over CES2, we studied CES1 activity in live HepG2 cells. This cell line was chosen as they express both CES1 and CES2.[26–28] Treating HepG2 cells with 2.5 μM FCP-1 resulted in a robust fluorescent signal after 15 minutes (Figure 3 and S4). Pretreatment of HepG2 cells with CES1 inhibitor troglitazone[29,30] resulted in a decrease of *ca.* 60% of fluorescence intensity (Figure 3A,B, and S4). Conversely, treatment with CES2 inhibitor loperamide[30,31] resulted in no significant change of fluorescence (Figure 3C,D, and S5). To confirm these results, we also knocked down CES1 and CES2 expression in HepG2 cells. Incubating CES1 shRNA-treated HepG2 cells with FCP-1 resulted in a decrease in fluorescence intensity by *ca.* 60% (Figure 3E,F and S6). Congruent with the CES2 inhibition studies, knocking down CES2 expression with shRNA had no influence on FCP-1 fluorescence in live cells (Figure 3G,H and S7). Overall, these results indicate that FCP-1 can specifically report on CES1 activity over CES2 in live cells.

Given that FCP-1 could report on CES1 activity in live cells, we next sought to use FCP-1 to develop a method to determine the activity differences caused by CES1 sequence variations. Current approaches that have been reported involve the stable expression of CES1 sequence variants in Flp-In-293 cells.[32–36] The lysates of these cells are then treated with known CES1 drug substrates and the hydrolysis by CES1 sequence variants is monitored by liquid chromatography methods. The time-consuming step of generating cell lines with stable expression is required in this method as the inclusion of cells that are not expressing CES1 sequence variants would result in an apparent decrease in CES1 activity. The use of FCP-1 could provide an alternative to stable cell lines as fluorescence microscopy provides spatial information which can be utilized to select only cells that are expressing the desired protein.[1,16] Therefore, we applied FCP-1 to develop an approach that can exploit this benefit of fluorescence microscopy.

To eliminate the requirement to use cells that have stable overexpression of CES1, we instead transiently co-transfected HEK293T cells with a mCherry2 expression plasmid and a CES1 expression plasmid. This common technique to express two different proteins in the same cell[37,38] allows the use of the image processing software like ImageJ[39] to select only the cells that are expressing the CES1 sequence variant of interest for analysis by operating under the assumption that cells that express mCherry2 are also expressing CES1 (Figure 4A). The HEK cell line was chosen for these studies as they are known to have

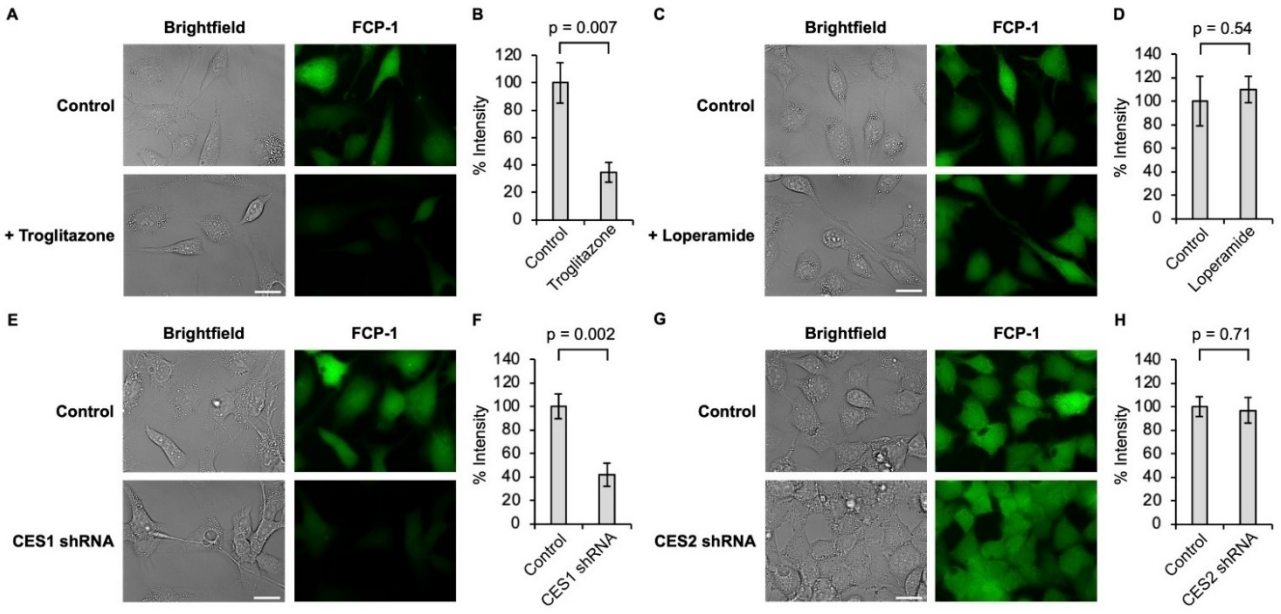

Figure 3. Fluorescence imaging of FCP-1 in live HepG2 cells. For inhibition studies, cells were treated with A. DMSO (control) or 50 μM troglitazone for 30 min or C. DMSO (control) or 50 μM loperamide for 30 min before loading with 2.5 μM FCP-1 for 15 minutes and imaged. B. Quantification of fluorescence signal of experiment described in A. D. Quantification of fluorescence signal of experiment described in C. For genetic knockdown studies, cells were transfected with scrambled shRNA vector (control) or a vector generating shRNA targeting E. CES1 (CES1 shRNA) or G. CES2 (CES2 shRNA) for 48 h before loading with 2.5 μM FCP-1 for 15 minutes and imaged. F. Quantification of fluorescence signal of experiment described in E. H. Quantification of fluorescence signal of experiment described in G. Scalebar = 20 μm. Error bars are ± std. dev. (n = 3).

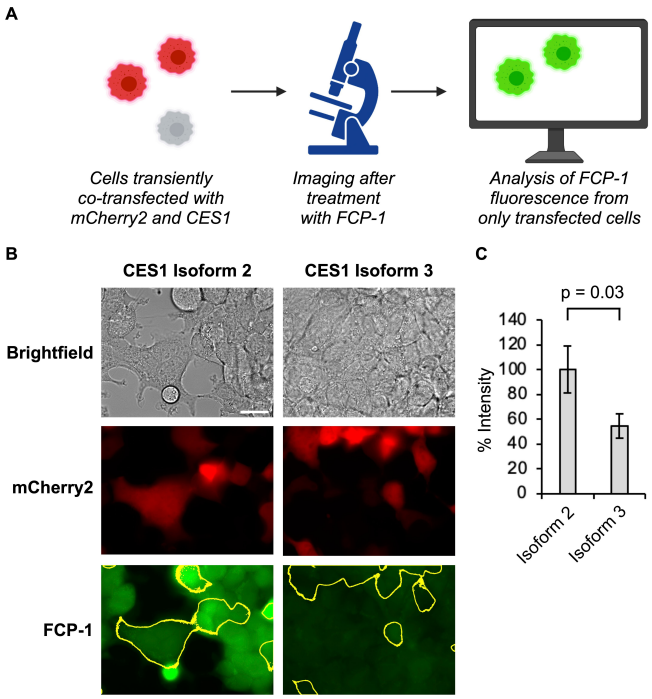

Figure 4. Fluorescence imaging of CES1 sequence variants. A. Diagram of the method developed to measure activity differences caused by CES1 sequence variations. Cells are co-transfected with mCherry2 and CES1 isoforms before being treated with FCP-1 and imaged by fluorescence microscopy in both the mCherry2 and FCP-1 channels. Imaging analysis software is used to only analyze FCP-1 signal in cells that were expressing mCherry2. B. Cells were co-transfected with mCherry2 vector and CES1 isoform 2 vector or mCherry2 vector and CES1 isoform 3 vector for 48 h before loading with 2.5 μM FCP-1 for 15 minutes and imaged with red (mCherry2) and green (FCP-1) filter sets. C. Quantification of fluorescence signal of experiment described in B. Only cells that expressed mCherry2 were selected for analysis (ROIs highlighted in yellow). Scalebar = 20 μm. Error bars are ± std. dev. (n = 3).

low levels of CES1 and CES2 expression and were used in previously reported stable expression methods.[26,32–36] To initially evaluate if this approach is viable, we co-transfected cells with mCherry2 and the canonical isoform of CES1 (isoform 2; Figure S8).[32] Treatment of these cells with FCP-1 resulted in a *ca.* 50% increase in fluorescence signal as compared to cells only transfected with the mCherry2 plasmid (Figure S9 and S10). This established that we could detect CES1 activity from transiently overexpressed CES1 in HEK293T cells.

Subsequently, we deployed this method to measure differences in CES1 activity caused by sequence variations. CES1 isoform 3 varies from the canonical isoform sequence of CES1 isoform 2 by having a single amino acid deleted (ΔQ362, Figure S8). Treating HEK293T cells overexpressing CES1 isoform 3 with FCP-1 resulted in *ca.* 50% less hydrolysis of FCP-1 compared to HEK293T cells overexpressing CES1 isoform 2 (Figure 4, S10, and S11). These results are consistent with a previous study[32] carried out in lysates using a stable expression method. This demonstrates that our approach can be utilized to study the influence of sequence variations on CES1 activity in live cells.

Conclusions

In conclusion, we have developed a new strategy for generating fluorescent chemical tools capable of reporting on CES1 activity in live cells. This approach has allowed for the use of a commercially available fluorophore and reagents to generate a new fluorescent chemical tool for CES1, FCP-1. This tool was shown to preferentially respond to endogenous CES1 activity in live cells with a robust fluorescent response. Deploying FCP-1 to develop an assay to measure the variability of activity between two overexpressed CES1 isoforms in live cells resulted in a novel method to use a fluorescent chemical tool to measure activity of CES1 amino acid sequence variants in live cells. We expect the approach reported here will prove to be valuable in annotating the activity of CES1 sequence variants leading to discovery of additional sequences that could result in abnormally low metabolism of CES1-substrate drugs.

Experimental Section

Synthesis of FCP-1 (6′-[(ethoxycarbonyl)oxy]-3-oxo-3*H*-spiro[2-benzofuran-1,9′-xanthen]-3′-yl ethyl carbonate): FCP-1 was synthesized according to a modified reported procedure.[40] Fluorescein (0.2092 g, 0.6298 mmol) was dissolved in 10 mL THF containing triethylamine (0.18 mL,1.3 mmol) in a 50 mL flame dried one neck round bottom flask equipped with a magnetic stir bar and sealed with a rubber septa under a nitrogen atmosphere. The solution was cooled to 0 °C in an ice bath followed by the dropwise addition of ethyl chloroformate (0.18 mL, 1.9 mmol). The solution was allowed to warm to room temperature overnight and concentrated under reduced pressure to yield the crude product. The product was purified via gradient silica column purification (100% hexanes to 30% EtOAc in hexanes) yielding 0.2517 g (83.9% yield) of a white solid. 1H NMR (400 MHz, DMSO-d6) δ (ppm): 8.08 (d, J = 7.2 Hz, 1H), 7.80 (m, 2H), 7.42 (m, 3H), 7.07 (d, J = 2 Hz, 1H), 7.05 (d, J = 2 Hz, 1H), 6.92 (s, 1H), 6.90 (s, 1H), 4.28 (q, J = 8 Hz, 4H), 1.30 (t, J = 8 Hz, 6H). 13C NMR (100 MHz, DMSO-d6) δ (ppm): 168.36, 152.37, 152.14, 152.11, 150.77,136.02, 130.59, 129.27, 125.37, 125.05, 124.12, 118.04, 116.43, 110.01, 80.80, 65.00, 13.93. HRA-MS(+) calculated for formula $C_{26}H_{20}O_9$ 476.1107; found 476.1110.

Solution stability at pH 7.4: 1 μM FCP-1, fluorescein diacetate (FDA), and fluorescein were incubated at room temperature in 1X PBS (Fisher) at pH 7.4 for 3 h with the fluorescence intensity (λ_{ex} = 488 nm, bandwidth = 1 nm; λ_{ex} = 512 nm, bandwidth = 8 nm) recorded every 1 min in triplicate.

Solution stability at variable pH: 1 μM FCP-1, FDA, and fluorescein with 0.1% DMSO were prepared in 20 mM glycine (pH 2.0–3.0),[41] acetate (pH 4.0–5.0),[41] phosphate (pH 6.0–8.0),[42] Tris (pH 9.0),[42] or CAPS (pH 10.0)[41] buffer and incubated for 30 min at 37 °C. After incubation, the fluorescence intensity (λ_{ex} = 488 nm, bandwidth = 1 nm; λ_{ex} = 512 nm, bandwidth = 8 nm) was recorded in triplicate.

***In vitro* FCP-1 and FDA hydrolysis by recombinant enzymes**: The units per μL of human recombinant enzyme CES1 (E0287-1VL Sigma-Aldrich, St. Louis, MO) and CES2 (E0412-1VL Sigma-Aldrich) were determined using the manufacture's protocol. FCP-1 or FDA were added to 500 μL of PBS containing 1.7 units of CES1 or CES2 at 37 °C at a final concentration of 1 μM with 0.1% DMSO. Every minute after addition for 180 minutes, the fluorescence intensity (λ_{ex} = 488 nm, bandwidth = 1 nm; λ_{ex} = 512 nm, bandwidth = 8 nm) was recorded.

Cell culture conditions: HepG2 and HEK293T cell lines were a gift from Dr. Bryan C. Dickinson (University of Chicago) and were maintained in DMEM/High Glucose (10% FBS, 1% Anti-Anti, Glutamax, sodium pyruvate, Gibco brand, Fisher) with 10% FBS (Benchmark line, GeminiBio, West Sacramento, CA) at 37 °C and 5% CO_2. Cells were used for less than 30 passages for all experiments.

General live cell fluorescence microscopy considerations: Fluorescence microscopy images were obtained on a Leica inverted fluorescence (epifluorescence) DM IL LED microscope equipped with an 60x oil objective. Red channel images were obtained using a Semrock mCherry-40LP–A Brightline Long Pass Filter Set (λ_{ex} = 530 nm to 590 nm; dichroic mirror = 590 nm; $\lambda_{em} \geq 600$ nm). Green channel images were obtained using a Semrock YFP-2427B Brightline Long Pass Filter Set (λ_{ex} = 480 nm to 510 nm; dichroic mirror = 510 nm; $\lambda_{em} \geq 560$ nm). All images were taken using identical conditions (exposure time, light source intensity, digital gain, and magnification) in relation to the relevant control conditions. Images were analyzed using ImageJ.[39] Image analysis was carried out on three different fields of view (n = 3) for each condition.

Live cell fluorescence imaging of FCP-1 with small molecule inhibitor: Four chamber glass bottom dishes (D35C4-20-1-N, Cellvis, Mountain View, CA) were coated with 300 μL poly-D-lysine (Gibco brand, Fisher) per chamber for an hour at room temperature or overnight at 4 °C, followed by washing with 500 μL of DPBS (Gibco brand, Fisher) twice. To each well, HepG2 cells were added in 750 μL of DMEM/High Glucose and incubated overnight to produce 70–80% confluency. The following day, the media was replaced with 500 μL of imaging solution (Gibco FluoroBrite DMEM supplemented with 20 mM HEPES, pH 7.4) containing either 50 μM Troglitazone, 50 μM Loperamide, or 0.1% DMSO (control). After incubation at 37 °C for 30 min, the solution was removed and cells were washed with 500 μL of DPBS followed by the addition of 500 μL of 2.5 μM FCP-1 in fresh imaging solution containing the appropriate inhibitor or DMSO. After 15 min incubation at 37 °C, the cells were washed with 500 μL of DPBS followed by the addition of 500 μL of fresh imaging solution containing the appropriate inhibitor or DMSO. The cells were then immediately imaged. Fluorescence was quantified my measuring total fluorescence signal in the green (FCP-1) channel over background using the threshold feature of ImageJ. Any oversaturated pixels were excluded in quantification of fluorescence signal.

Live cell fluorescence imaging of FCP-1 with shRNA: HepG2 cells were added in 750 μL of DMEM/High Glucose to each well of a lysine coated four chamber glass bottom dish and incubated overnight to a confluency of 70% to 80%. The next day cells were transfected with 0.7 μg of CES1 shRNA plasmid (target sequence: CGGAATTAAC AAGCAGGAGTT, TRCN0000046933,), CES2 shRNA plasmid (target sequence: CAGCAGAATA TCGCCCACTTT, TRCN0000046964), or scrambled shRNA plasmid (gift from David Sabatini)[43] using 6 μL Transporter 5 Transfection Reagent (Polysciences, Warrington, PA) with a final volume of 150 μL in Opti-MEM (Gibco brand, Fisher) in serum and antibiotic-free DMEM/Glucose media according to the manufacture's protocol. After 6–12 h, the media was replaced with DMEM/High Glucose. Following 48 h incubation at 37 °C and 5% CO2, media was removed, cells were washed with 500 μL of DPBS. And the solution was then replaced with 500 μL of imaging solution containing 2.5 μM FCP-1 with 0.05% DMSO. After 15 min incubation at 37 °C, the solution was removed, cells washed with 500 μL of DPBS and 500 μL of fresh imaging solution was placed in each well before immediately imaging the cells. Fluorescence was quantified my measuring total fluorescence signal in the green (FCP-1) channel over background using the threshold feature of ImageJ. Any oversaturated pixels were excluded in quantification of fluorescence signal.

Comparison of CES1 isoform activity in HEK293T cells: HEK293T cells were added in 750 μL of DMEM/High Glucose to each well of a lysine coated four chamber glass bottom dish and incubated overnight to produce 70–80% confluency. The next day cells were transfected with 0.7 μg of mCherry2-N1 and 0.7 μg d0-CES1 isoform 2 or 0.7 μg of mCherry2-N1 and 0.7 μg d0-CES1 isoform 3 using 6 μL Transporter 5 Transfection Reagent with a final volume of 150 μL in Opti-MEM (Gibco, Fisher) in serum and antibiotic-free DMEM/Glucose media according to the manufacture's protocol. After 6–12 h, the media was replaced with DMEM/High Glucose. Following 48 h incubation at 37 °C and 5% CO_2, media was removed, cells were washed with 500 μL DPBS and the solution was then replaced with 500 μL of imaging solution containing 2.5 μM FCP-1 with 0.05% DMSO. After 15 min incubation at 37 °C, the solution was removed, cells washed with 500 μL of DPBS and 500 μL of fresh imaging solution was placed in each well before immediately imaging the cells. Analysis of the fluorescence intensity was only performed on cells expressing mCherry2. To avoid biasing the results, this was performed by including all regions of mCherry2 signal above background using the auto threshold feature of ImageJ. Any oversaturated pixels were excluded in quantification of fluorescence signal.

Statistics: All errors reported as +/− standard deviation. p-values were calculated using a heteroscedastic two-tailed Student's t-Test.

Acknowledgements

This work was supported by EIU Department of Chemistry and Biochemistry, EIU Student Impact Grant for Faculty Mentors to M.W.B., EIU Summer Creative Activity/Research Award to M.W.B, and EIU Graduate School Creative/Research Activity Award to A.S. A.S. also thanks the EIU Department of Chemistry and Biochemistry and EIU Graduate School for their support through a graduate assistantship. Generous funding from the National Science Foundation was used to purchase the Edinburgh Instruments FS5 spectrofluorometer (NSF 1507871) and the Bruker Advance 400 MHz spectrometer (NSF 0321321). Figure 1 and Figure 4A were created with BioRender.com.

Conflict of Interest

The authors declare no conflict of interest.

Data Availability Statement

The data that support the findings of this study are available in the supplementary material of this article.

Keywords: carboxylesterases · fluorescence microscopy · fluorescent probes · hydrolases · imaging agents

[1] A. Singh, M. Gao, M. W. Beck, *RSC Med. Chem.* **2021**, *12*, 1142–1153.
[2] R. S. Holmes, M. W. Wright, S. J. F. Laulederkind, L. A. Cox, M. Hosokawa, T. Imai, S. Ishibashi, R. Lehner, M. Miyazaki, E. J. Perkins, P. M. Potter, M. R. Redinbo, J. Robert, T. Satoh, T. Yamashita, B. Yan, T. Yokoi, R. Zechner, L. J. Maltais, *Mamm. Genome* **2010**, *21*, 427–441.
[3] Y. Shen, W. Eades, B. Yan, *Hepatol. Commun.* **2021**, *5*, 1622–1623.

[4] R. Li, A. Liclican, Y. Xu, J. Pitts, C. Niu, J. Zhang, C. Kim, X. Zhao, D. Soohoo, D. Babusis, Q. Yue, B. Ma, B. P. Murray, R. Subramanian, X. Xie, J. Zou, J. P. Bilello, L. Li, B. E. Schultz, R. Sakowicz, B. J. Smith, P.-Y. Shi, E. Murakami, J. Y. Feng, *Antimicrob. Agents Chemother.* **2021**, *65*, e0060221.
[5] L. Her, H. J. Zhu, *Drug Metab. Dispos.* **2020**, *48*, 230–244.
[6] L. Di, *Curr. Drug Metab.* **2019**, *20*, 91–102.
[7] S. Casey Laizure, V. Herring, Z. Hu, K. Witbrodt, R. B. Parker, *Pharmacotherapy* **2013**, *33*, 210–222.
[8] Z. Tian, L. Ding, K. Li, Y. Song, T. Dou, J. Hou, X. Tian, L. Feng, G. Ge, J. Cui, *Anal. Chem.* **2019**, *91*, 5638–5645.
[9] L. Ding, Z. Tian, J. Hou, T. Dou, Q. Jin, D. Wang, L. Zou, Y. Zhu, Y. Song, J. Cui, G. Ge, *Chin. Chem. Lett.* **2019**, *30*, 558–562.
[10] C. Ma, J. Wu, W. Sun, Y. Hou, G. Zhong, R. Gao, B. Shen, H. Huang, *Sens. Actuators B* **2020**, *325*, 128798.
[11] S. Kim, J. Bouffard, Y. Kim, *Chem. Eur. J.* **2015**, *21*, 17459–17465.
[12] R. Hua, P. K. Kim, *Biochim. Biophys. Acta Mol. Cell Res.* **2016**, *1863*, 881–891.
[13] Y.-Q. Song, Q. Jin, D.-D. Wang, J. Hou, L.-W. Zou, G.-B. Ge, *Chem.-Biol. Interact.* **2021**, *345*, 109566.
[14] A. Alouane, R. Labruère, T. Le Saux, F. Schmidt, L. Jullien, *Angew. Chem. Int. Ed.* **2015**, *54*, 7492–7509; *Angew. Chem.* **2015**, *127*, 7600–7619.
[15] L. D. Lavis, R. T. Raines, *ACS Chem. Biol.* **2014**, *9*, 855–866.
[16] W. Chyan, R. T. Raines, *ACS Chem. Biol.* **2018**, *13*, 1810–1823.
[17] Y. Fu, N. S. Finney, *RSC Adv.* **2018**, *8*, 29051–29061.
[18] L. D. Lavis, R. T. Raines, *ACS Chem. Biol.* **2008**, *3*, 142–155.
[19] W. Chyan, H. R. Kilgore, B. Gold, R. T. Raines, *J. Org. Chem.* **2017**, *82*, 4297–4304.
[20] L. D. Lavis, *Biochemistry* **2021**, *60*, 3539–3546.
[21] S. Smith, W. Pretorius, *Water SA* **2002**, *28*, 395–402.
[22] K. I. O'goshi, J. Serup, *Ski. Res. Technol.* **2006**, *12*, 155–161.
[23] J. Wang, E. T. Williams, J. Bourgea, Y. N. Wong, C. J. Patten, *Drug Metab. Dispos.* **2011**, *39*, 1329–1333.
[24] D. L. Kroetz, F. J. Gonzalez, O. W. McBride, *Biochemistry* **1993**, *32*, 11606–11617.
[25] V. Arena de Souza, D. J. Scott, J. E. Nettleship, N. Rahman, M. H. Charlton, M. A. Walsh, R. J. Owens, *PLoS One* **2015**, *10*, e0143919.
[26] S. E. Pratt, S. Durland-Busbice, R. L. Shepard, K. Heinz-Taheny, P. W. Iversen, A. H. Dantzig, *Clin. Cancer Res.* **2013**, *19*, 1159–1168.
[27] W. Luo, Y. Xin, X. Zhao, F. Zhang, C. Liu, H. Fan, T. Xi, J. Xiong, *Br. J. Pharmacol.* **2017**, *174*, 700–717.
[28] W. Shang, J. Liu, R. Chen, R. Ning, J. Xiong, W. Liu, Z. Mao, G. Hu, J. Yang, *Xenobiotica* **2016**, *46*, 393–405.
[29] T. Fukami, S. Takahashi, N. Nakagawa, T. Maruichi, M. Nakajima, T. Yokoi, *Drug Metab. Dispos.* **2010**, *38*, 2173–2178.
[30] Z. Feng, H. Wang, R. Zhou, J. Li, B. Xu, *J. Am. Chem. Soc.* **2017**, *139*, 3950–3953.
[31] S. K. Quinney, S. P. Sanghani, W. I. Davis, T. D. Hurley, Z. Sun, D. J. Murry, W. F. Bosron, *J. Pharmacol. Exp. Ther.* **2005**, *313*, 1011–1016.
[32] X. Wang, J. Shi, H.-J. Zhu, *Proteomics* **2019**, *19*, e1800288.
[33] H.-J. Zhu, X. Wang, B. E. Gawronski, B. J. Brinda, D. J. Angiolillo, J. S. Markowitz, *J. Pharmacol. Exp. Ther.* **2013**, *344*, 665–672.
[34] X. Wang, N. Rida, J. Shi, A. H. Wu, B. E. Bleske, H.-J. Zhu, *Drug Metab. Dispos.* **2017**, *45*, 1149–1155.
[35] X. Wang, G. Wang, J. Shi, J. Aa, R. Comas, Y. Liang, H.-J. Zhu, *Pharmacogenomics J.* **2016**, *16*, 220–230.
[36] J. Shi, X. Wang, J. Nguyen, A. H. Wu, B. E. Bleske, H.-J. Zhu, *Drug Metab. Dispos.* **2016**, *44*, 554–559.
[37] Z. Xie, S. Shao, J. Lv, C. Wang, C. Yuan, W. Zhang, X. Xu, *Cell Biol. Int.* **2011**, *35*, 187–192.
[38] S. Sugita, *Methods* **2004**, *33*, 267–272.
[39] J. Schindelin, I. Arganda-Carreras, E. Frise, V. Kaynig, M. Longair, T. Pietzsch, S. Preibisch, C. Rueden, S. Saalfeld, B. Schmid, J. Y. Tinevez, D. J. White, V. Hartenstein, K. Eliceiri, P. Tomancak, A. Cardona, *Nat. Methods* **2012**, *9*, 676–682.
[40] Y. Yue, F. Huo, C. Yin, *Anal. Chem.* **2019**, *91*, 2255–2259.
[41] R. Ohgaki, Y. Teramura, D. Hayashi, L. Quan, S. Okuda, S. Nagamori, M. Takai, Y. Kanai, *Sci. Rep.* **2017**, *7*, 17484.
[42] M. Martineau, A. Somasundaram, J. B. Grimm, T. D. Gruber, D. Choquet, J. W. Taraska, L. D. Lavis, D. Perrais, *Nat. Commun.* **2017**, *8*, 1412.
[43] D. D. Sarbassov, D. A. Guertin, S. M. Ali, D. M. Sabatini, *Science.* **2005**, *307*, 1098–1101.

Manuscript received: February 1, 2022
Revised manuscript received: March 5, 2022
Accepted manuscript online: March 7, 2022
Version of record online: ■■, ■■■

RESEARCH ARTICLE

Despite the established importance of carboxylesterase 1 (CES1) in drug metabolism, methods to monitor factors that influence CES1 activity are limited. Herein, we exploit the self-immolative properties of carbonates to generate a fluorescent chemical tool and use it to identify activity differences between CES1 sequence variants in live cells.

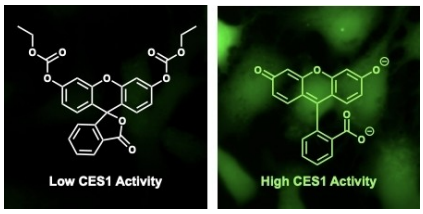

*A. Singh, M. Gao, C. J. Karns, T. P. Spidle, Prof. Dr. M. W. Beck**

1 – 7

Carbonate-Based Fluorescent Chemical Tool for Uncovering Carboxylesterase 1 (CES1) Activity Variations in Live Cells